ISSN 1330-3651 (Print), ISSN 1848-6339 (Online)
DOI: 10.17559/TV-20140423164817

COMPARISON OF USAGE OF DIFFERENT NEURAL STRUCTURES TO PREDICT AAO LAYER THICKNESS

Alena Vagaská, Miroslav Gombár

Original scientific paper
The paper deals with the comparison of usage of three basic types of neural units in order to create the most suitable model predicting determining the final thickness of the alumina layer formed at surface with current density of 1 A·dm^{-2}. In addition, the reliability of obtained prediction models, depending on the amount of training data, has been monitored. With properly selected range of training data it is possible to create prediction models with reliability greater than 95 % with achieved toleration 2×10^{-6} mm.

Keywords: *anodizing; neural unit; prediction model*

Usporedba primjene raznih neuralnih struktura u predviđanju debljine sloja anodnog aluminij oksida

Izvorni znanstveni članak
Rad se bavi usporedbom uporabe triju osnovnih vrsta neuralnih jedinica u cilju stvaranja najprikladnijeg modela koji predviđa utvrđivanje konačne debljine sloja aluminijeva oksida koji nastaje na površini uz gustoću struje od 1 A·dm^{-2}. Osim toga, prati se pouzdanost dobivenih modela predviđanja, ovisno o količini podataka za vježbu. Uz pravilno odabrani raspon podataka za vježbu moguće je stvoriti modele predviđanja s pouzdanošću većom od 95 % s postignutom tolerancijom 2×10^{-6} mm.

Ključne riječi: *eloksiranje; neuralna jedinica; model predviđanja*

1 Introduction

Pure aluminium and its alloys, as weight-reducing materials, are becoming more significant not only from technical, but also from technological and economic standpoint [1], [2] mostly in aerospace and automobile industries, where light and sturdy structures are preferred [3], [4]. Using these materials for moving parts presents a great challenge when high resistance to abrasion and wear is required [5]. These tribological properties can be improved by anodic oxidation of components surface. Anodizing is one of the most important processes in corrosion protection and colour finishes for aluminium [6]. Design of experiments (DoE) is one of the basic tools which help us to show the influence of input factors on outputs [7-10]. The optimum selection of process conditions is an extremely important issue as these determine surface quality of the manufactured components [11-13]. The mathematical modelling of the process involves several parameters that may lead to difficult analytical solution [14], [15]. On the other hand, use of artificial intelligence for evaluation of experiments results has its merits mainly because of faster and more reliable creation of prediction model for the studied process, compared to classic statistical methods [16-19].

2 Methods

Based on DoE, we have oxidized 46 samples of alloy EN AW 1050A. Chemical composition of electrolytes was in accordance with central composite design of experiment. Composition of electrolyte was influenced by amount of sulphuric acid in electrolyte (factor x_1), amount of oxalic acid in electrolyte (factor x_2) and amount of aluminium cations in electrolyte (factor x_3). Operating conditions were: electrolyte temperature (factor x_4), time of oxidation (factor x_5) and applied voltage level (factor x_6). Naming of observed factors and their levels in natural and coded scale are shown in Tab. 1.

Table 1 Factors level in nature and coded scale

Factor		Factor level				
Code scale	Natural scale	−2,37	−1	0	+1	+2,37
x_1	H_2SO_4/ g·l^{-1}	33,51	130,0	200,0	270,0	366,5
x_2	$C_2H_2O_4$/ g·l^{-1}	1,49	7,0	11,0	15,0	20,51
x_3	Al^{3+}/ g·l^{-1}	0,18	5,0	8,5	12,0	16,82
x_4	T/ °C	−1,78	12,0	22,0	32,0	45,78
x_5	t/ min	6,22	20,0	30,0	40,0	53,78
x_6	U/ V	5,24	8,0	10,0	12,0	14,76

We have measured the thickness of aluminium oxide layer on each sample after the oxidation. Layer thickness was measured in the area with surface current density 1 A·dm^{-2}.

We have used three types of neural units to compile prediction model: 1st order HONU (**H**igher-**O**rder **N**eural **U**nit) (linear neuron unit), 2nd order HONU (quadratic neural unit) and 3rd order HONU (cubic neuron unit). These neural units compiled the prediction model based on adaptive optimization algorithm - Levenberg-Marquardt [20], [21].

This algorithm is described by Eq. (1) ÷ (8). It is a process of updating individual weights w in a predetermined number of steps to achieve a minimum difference between the real (measured) and calculated values. The vector u of neural inputs is created by taking the partial derivatives of each output in respect to each weight Eq. (1) – Eq. (3). The equation describing the investigated model is the characteristic equation of given type of neural unit (1st order HONU, 2nd order HONU a 3rd order HONU) for observed factors x_1, x_2, x_3, x_4, x_5, x_6 [22], [23].

$$u_i = \frac{\partial y_{\mathrm{HONU}}}{\partial w_i} \tag{1}$$

$$\mathbf{u} = \begin{bmatrix} u_1 \\ u_2 \\ \vdots \\ u_n \end{bmatrix} \tag{2}$$

$$\mathbf{w} = \begin{bmatrix} w_1 \\ w_2 \\ \vdots \\ w_n \end{bmatrix} \tag{3}$$

The Levenberg-Marquardt algorithm consists of solving Eq. (4), where the Jacobian $\boldsymbol{J}$ is the matrix of dimension $n \times m$, where n is the length of the input vector $\boldsymbol{u}$ of the neural unit (n is the number of neural inputs) and m is the total number of parameters intended for the learning procedure.

$$\boldsymbol{J} = \begin{bmatrix} \boldsymbol{u}_1^{\mathrm{T}} \\ \boldsymbol{u}_2^{\mathrm{T}} \\ \vdots \\ \boldsymbol{u}_m^{\mathrm{T}} \end{bmatrix} = \begin{bmatrix} u_{1;1} & u_{2;1} & \cdots & u_{n;1} \\ u_{1;2} & u_{2;2} & \cdots & u_{n;2} \\ \vdots & \vdots & \ddots & \vdots \\ u_{1;m} & u_{2;m} & \cdots & u_{n;m} \end{bmatrix} \tag{4}$$

The vector $\boldsymbol{y'}$ of neural outputs is defined as the dot product of vectors $\boldsymbol{w}$ and $\boldsymbol{u}$ Eq. (5), the size of the individual weight is set in the first step randomly.

$$\boldsymbol{y'} = \boldsymbol{w} \cdot \boldsymbol{u} \tag{5}$$

After calculating the output vector, the error vector $\boldsymbol{e}$ is calculated as the difference between the actual value $\boldsymbol{y}$ of the observed variable and the calculated one by the neural units $\boldsymbol{y'}$, as seen in Eq. (6).

$$\boldsymbol{e} = \boldsymbol{y} - \boldsymbol{y'} \tag{6}$$

Then the weight update vector $\boldsymbol{\Delta w}$ is determined by Eq. (7). In Eq. (7) is the weight update vector $\boldsymbol{\Delta w}$ that we want to find, e is the error vector containing the output errors for each input vector used on training the network, $1/\mu$ is the Levenberg's damping factor which tells us by how much we should change our network weights to achieve a (possibly) better solution. The $\boldsymbol{J}^{\mathrm{T}} \cdot \boldsymbol{J}$ matrix can also be known as the approximated Hessian, the $\boldsymbol{I}$ is an identity matrix of diagonal length equal to the number of neural weights (matrix of dimension $n \times n$), and μ is the learning rate. The size of the learning rate μ depends on how quickly and how accurately the neural unit is able to learn.

$$\boldsymbol{\Delta w} = \left(\boldsymbol{J}^{\mathrm{T}} \cdot \boldsymbol{J} + \frac{1}{\mu} \cdot \boldsymbol{I} \right)^{-1} \cdot \boldsymbol{J}^{\mathrm{T}} \cdot \boldsymbol{e} \tag{7}$$

After calculating the weight-updates Eq. (8), the adaptation of the weights of input factors occurs. Weight update vector $\boldsymbol{\Delta w}$ is sum up to actual vector of weight w. The learning process of neural units continues by calculating the vector of neural outputs y using the new (adapted) weights.

$$\boldsymbol{w} = \boldsymbol{w} + \boldsymbol{\Delta w} \tag{8}$$

After the learning process of neuron unit is done, we get a computational model that describes the thickness of AAO layer with equation Eq. (9) and Eq. (10) for linear neural unit, Eq. (11) and Eq. (12) for quadratic neural unit and Eq. (13) and Eq. (14) for cubic neural unit.

$$th_{LNUth} = \frac{3}{1 + e^{-\alpha_{LNU}}} 3 \cdot std_y \tag{9}$$

$$\alpha_{LNU} = \sum_{i=1}^{n} (u_{iLNU} \cdot w_{iLNU}) \tag{10}$$

$$th_{QNU} = \frac{3}{1 + e^{-\alpha_{QNU}}} 3 \cdot std_y \tag{11}$$

$$\alpha_{QNU} = \sum_{i=1}^{n} (u_{iQNU} \cdot w_{iQNU}) \tag{12}$$

$$th_{CNU} = \frac{3}{1 + e^{-\alpha_{CNU}}} 3 \cdot std_y \tag{13}$$

$$\alpha_{CNU} = \sum_{i=1}^{n} (u_{iCNU} \cdot w_{iCNU}) \tag{14}$$

where th is final thickness of oxide layer, α is preliminary thickness of oxide layer, u_i is a combination of input factors levels (in coded scale), w_i are weights for combinations of input factors and std_y is standard deviation of real values (measured layer thickness vector $\boldsymbol{y}$) divided by 3. Calculated thickness of oxide layer is expressed in 10^{-3} mm.

3 Results

We have gradually reduced range of training data during the neural unit's learning process. At first, we have used all of the 46 measurements of AAO (anodic aluminium oxide) layer thickness. The number of AAO layer thickness values was reduced by one with each subsequent iteration of the learning process. The lowest range of training data was 10 measurements of thickness. Tab. 2 shows learning error (sum of square errors for learning process for linear neural unit - sse_{LLNU}, quadratic neural unit - sse_{LQNU} and cubic neural unit - sse_{LCNU}) for each neural unit in selected range of training data (number of training values - $NoTV$).

From shown sums of squared errors (Tab. 2), we can assume that each type of neural unit can produce more reliable prediction model with less training data.

However, process of verification denies this assumption.

Figs. 1 ÷ 3 show an error of predicted AAO layer thickness for linear, quadratic and cubic neural unit. Each neural unit used all of the 46 measurements of AAO layer thickness during the learning process.

Table 2 Learning error of neural units

NoTV	*LNU*	*QNU*	*CNU*
46	480,48	100,82	$8,83\times10^{-1}$
45	479,17	96,50	$8,56\times10^{-1}$
44	478,91	90,17	$8,40\times10^{-1}$
43	466,42	80,05	$8,29\times10^{-1}$
42	464,97	65,84	$8,24\times10^{-1}$
41	464,61	64,33	$5,48\times10^{-3}$
40	464,59	47,60	$2,21\times10^{-3}$
39	464,56	35,77	$1,67\times10^{-3}$
38	463,89	29,59	$1,02\times10^{-3}$
37	440,85	28,84	$1,94\times10^{-9}$
36	436,81	28,21	$6,62\times10^{-11}$
35	430,74	28,17	$9,74\times10^{-11}$
34	422,72	28,17	$8,96\times10^{-11}$
33	421,47	12,49	$1,20\times10^{-10}$
32	389,16	12,47	$1,85\times10^{-10}$
31	388,17	10,47	$4,22\times10^{-11}$
30	388,22	10,46	$7,08\times10^{-11}$
29	367,77	10,33	$6,66\times10^{-11}$
28	367,60	10,11	$1,25\times10^{-10}$
27	339,62	1,75	$2,73\times10^{-11}$
26	335,91	1,75	$5,67\times10^{-11}$
25	321,53	1,75	$6,46\times10^{-11}$
24	317,79	1,73	$2,08\times10^{-15}$
23	306,14	1,73	$5,23\times10^{-15}$
22	306,00	1,20	$1,63\times10^{-14}$
21	305,79	1,20	$5,50\times10^{-14}$
20	298,42	1,11	$5,70\times10^{-14}$
19	292,81	1,10	$1,74\times10^{-13}$
18	289,68	$1,93\times10^{-4}$	$1,17\times10^{-13}$
17	289,23	$2,13\times10^{-5}$	$1,12\times10^{-13}$
16	286,46	$2,65\times10^{-5}$	$5,55\times10^{-14}$
15	284,64	$2,55\times10^{-13}$	$1,26\times10^{-14}$
14	217,76	$1,53\times10^{-14}$	$1,89\times10^{-15}$
13	199,92	$1,41\times10^{-15}$	$1,21\times10^{-16}$
12	182,45	$7,22\times10^{-15}$	$6,91\times10^{-16}$
11	65,72	$6,65\times10^{-16}$	$9,96\times10^{-17}$
10	61,33	$8,83\times10^{-23}$	$1,04\times10^{-23}$

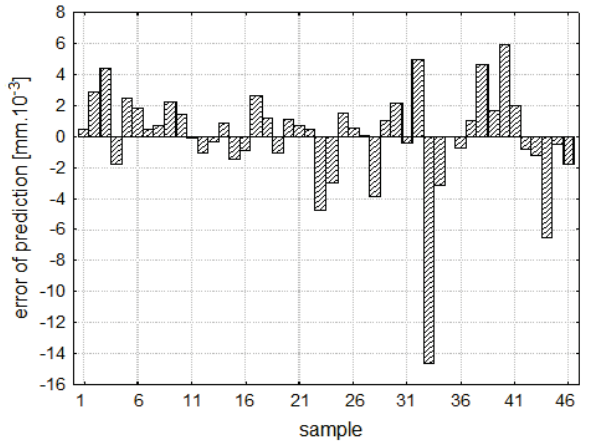

Figure 1 Validation of *LNU* for training process with 46 training data

Linear prediction model created by *LNU* (Fig. 1) is comparatively accurate because error of prediction is less than $\pm4,00\times10^{-3}$ mm for 39 samples. On the other hand error of prediction is greater than $4,00\times10^{-3}$ mm for 7 samples, especially for sample of number 33, where the prediction error is $14,50\times10^{-3}$ mm. Therefore, it is possible to use this prediction model only as indication to the AAO layer thickness. Use of this model for optimization of aluminium anodizing is impossible.

Fig. 2 shows that *QNU* was able to create a model with high prediction capability. We can see in Fig. 2 that 37 samples are in toleration area $\pm2,00\times10^{-3}$ mm. The other 6 samples are in toleration area $\pm3,00\times10^{-3}$ mm and finally 3 samples are in toleration area $\pm4,00\times10^{-3}$ mm. Therefore, it is possible to use this quadratic prediction model for optimization of anodic oxidation of aluminium but only under certain conditions. For example if the toleration area $\pm5,00\times10^{-3}$ mm is acceptable.

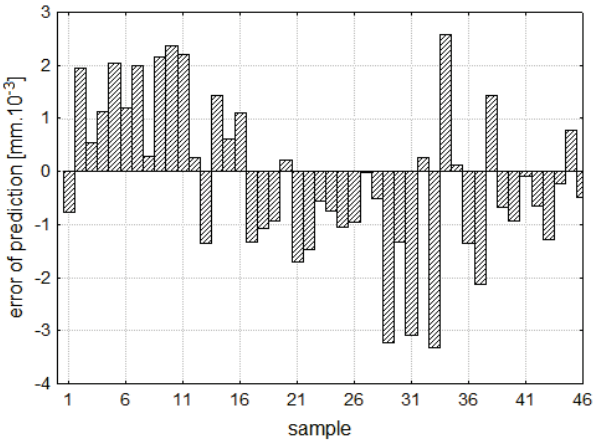

Figure 2 Validation of *QNU* for training process with 46 training data

Fig. 3 shows that *CNU* was able to create almost perfect prediction model. It can be seen that only 2 samples have error of computation $\pm0,60\times10^{-3}$ mm. All other samples have error of computation less than $0,20\times10^{-3}$ mm (mostly less than $0,05\times10^{-3}$ mm). It means that this *CNU* prediction model can be considered accurate. So it is possible to use this model to optimize process of aluminium anodizing.

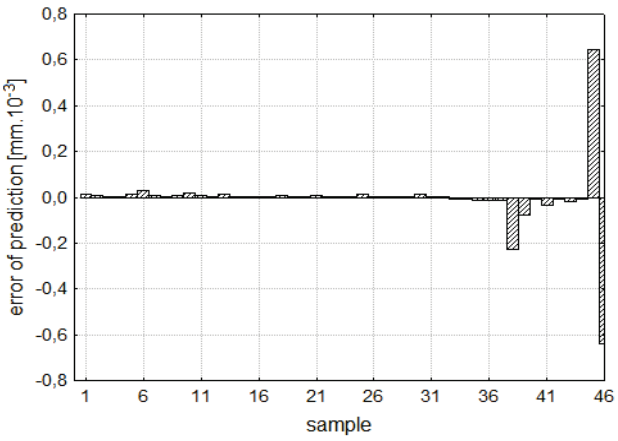

Figure 3 Validation of *CNU* for training process with 46 training data

If we use all measured layer thickness measurements in learning process it can be very difficult to determine if the prediction model is compiled correctly, because we do not have any measurements to validate the compiled prediction model. There is a risk of overtraining the neural unit. This is the reason why we have gradually reduced range of training data during the learning process.

Tab. 3 shows the sum of squared errors between measured and calculated values of AAO layer thickness for each neural unit. Generally it can be concluded from Tab. 3 that with decrease in amount of training data also

decreases the reliability of prediction of AAO layer thickness, but there are some exceptions.

Table 3 Sum of square errors for linear, quadratic and cubic neural unit

NoTV	*LNU*	*QNU*	*CNU*
46	480,48	100,82	0,88
45	480,84	111,85	29,83
44	481,09	121,11	43,93
43	485,38	180,15	58,92
42	486,10	311,36	45,21
41	486,50	308,47	32,52
40	486,39	521,96	21,24
39	486,59	2359,69	17,15
38	485,72	2722,17	14,18
37	487,51	3067,18	14,70
36	489,20	3032,19	8,63
35	494,30	1556,83	10,19
34	498,61	811,15	47,90
33	499,45	1302,69	47,72
32	496,90	1083,39	47,78
31	496,16	1407,58	47,46
30	495,83	1287,63	47,79
29	503,92	1096,19	47,72
28	504,11	1363,13	53,83
27	561,25	1839,04	281,30
26	548,93	2034,12	281,13
25	555,03	2100,54	283,84
24	554,35	1864,39	265,46
23	614,43	1954,48	284,75
22	611,99	2090,70	300,16
21	614,54	1982,23	307,26
20	620,31	909,05	306,27
19	640,38	916,27	335,56
18	649,77	544,30	326,12
17	648,20	441,43	322,85
16	655,43	471,22	320,80
15	664,16	657,03	328,32
14	126,12	793,33	615,62
13	1802,31	1028,14	774,67
12	2202,95	870,17	790,81
11	790,09	915,69	786,31
10	660,48	938,05	902,75

QNU has smaller error of prediction than *LNU* only if we use from 46 to 41 training values. Then the sum of square errors is rapidly increasing with each decrease of training data for *QNU*, until we reach 25 training data. After that the sum of squared errors for *QNU* starts decreasing again, until we reach 15 training data. Then it starts increasing.

Sum of square errors for *LNU* is relatively at constant level all the time. It gradually increases from 480 to 670 until we reached only 15 training data. If we use 10 or 11 training data for *LNU*, the prediction model is more precise than if we use more training data (12, 13 or 14).

The sum of squared errors for *CNU* is increasing from 0,8 (46 training data are used) to 59 (43 training data are used). Then it starts decreasing to 8,6 (36 training data are used). After that it is still increasing.

From Tab. 3 we can conclude that examined neural unit can compile very accurate prediction model if the sum of squared errors is ranging from 0,00 to 50,00. Prediction model is considered accurate if the sum of squared errors is ranging from 50,00 to 200,00. Prediction model can be used only for approximation if the sum of squared errors is ranging from 200,00 to 500,00. Prediction model is considered unusable with sum of squared errors greater than 500,00.

Fig. 4, Fig. 5 and Fig. 6 show an error between computed and measured AAO layer thickness for linear, quadratic and cubic neural units, which used 36 values of AAO layer thickness during their learning process.

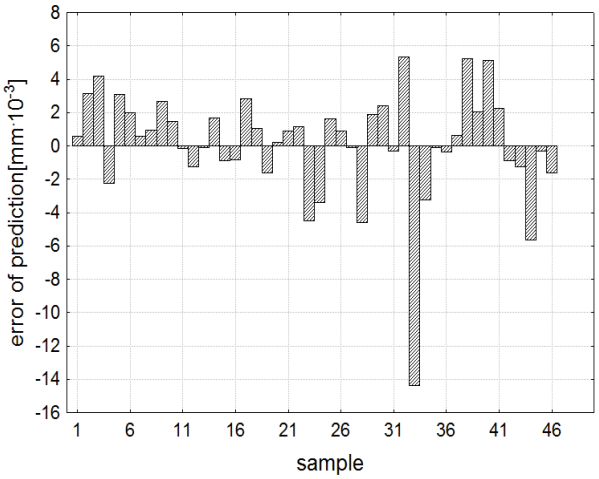

Figure 4 Validation of *LNU* for training process with 36 training data

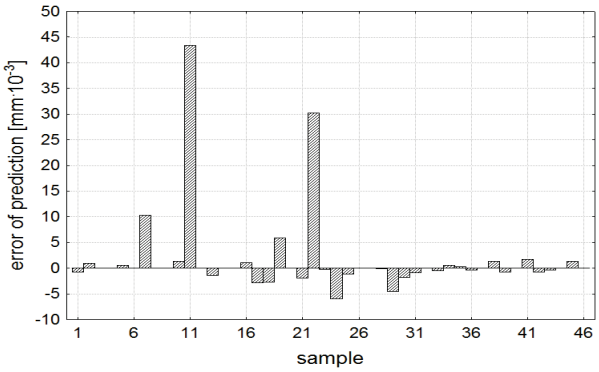

Figure 5 Validation of *QNU* for training process with 36 training data

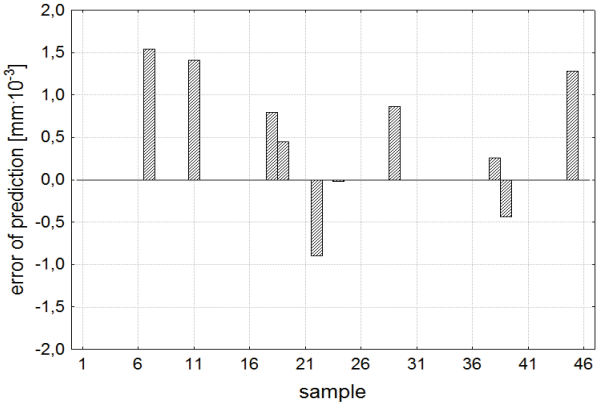

Figure 6 Validation of *CNU* for training process with 36 training data

Linear prediction model (Fig. 4) is still usable for approximate calculations. Error of prediction is less than $\pm 4{,}00\times10^{-3}$ mm for 37 samples and error of prediction is greater than $4{,}00\times10^{-3}$ mm for 9 samples. Fig. 5 shows that error for quadratic prediction model is too large (almost $45{,}00\times10^{-3}$ mm) for the model to be usable. Its accuracy is further reduced with a decrease in amount of training data. Cubic prediction model (Fig. 6) is still very reliable. Error of prediction is in toleration area

$\pm 1{,}50\times10^{-3}$ mm for 3 samples, in toleration area $\pm 0{,}50\times10^{-3}$ mm for 4 samples and error of prediction is 0,00 mm for other 36 samples.

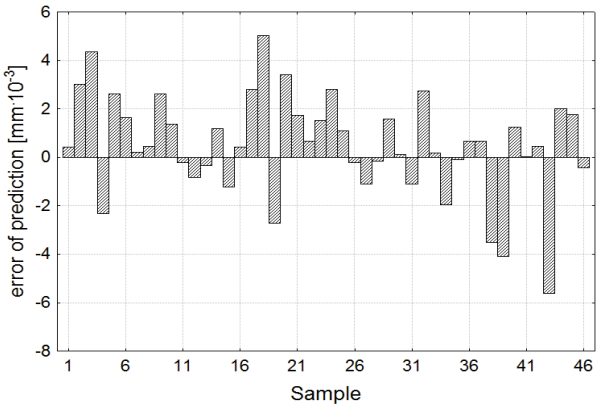

Figure 7 Validation of *LNU* for training process with 28 training data

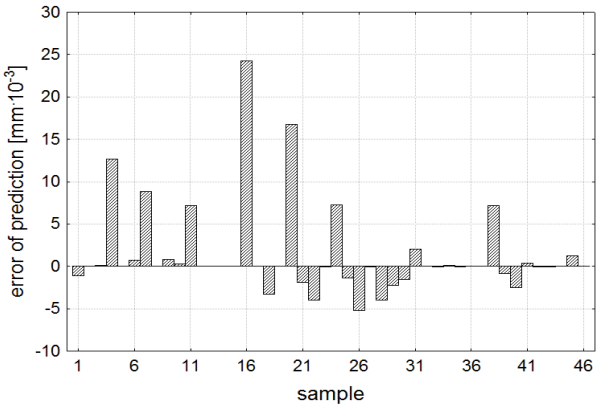

Figure 8 Validation of *QNU* for training process with 28 training data

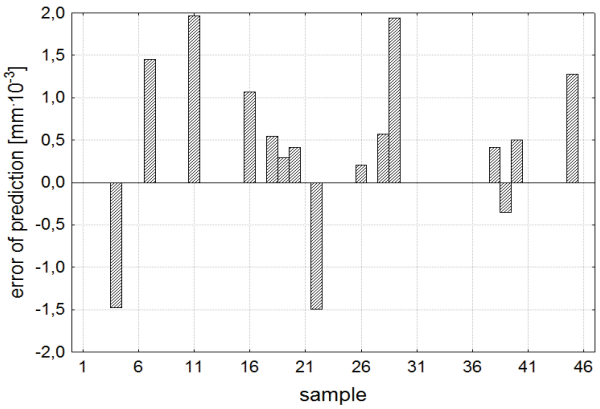

Figure 9 Validation of *CNU* for training process with 28 training data

Fig. 7, Fig. 8 and Fig. 9 show a comparison of measured and predicted AAO layer thickness for *LNU*, *QNU* and *CNU*, which used 28 values of AAO layer thickness during their learning process. As we can see from Fig. 7 *LNU* still has capability to compile an approximate predictive model. Error of prediction is usual in range $\pm 6{,}00\times10^{-3}$ mm, but it is mostly in range $\pm 2{,}00\times10^{-3}$ mm. The prediction model compiled by *QNU* which use 28 training data (Fig. 8) is unusable the same as in previous case. As shown in Fig. 8, error for quadratic prediction model is too large (almost $25{,}00\times10^{-3}$ mm) for the model to be usable. Its accuracy is further reduced with a decrease in amount of training data. As shown in Fig. 9, cubic prediction model compiled by *CNU* is still very precision again Every error of prediction is in toleration area $\pm 2{,}00\times10^{-3}$ mm. But this is last time when the cubic prediction model is usable to optimize the examined process of anodizing.

Fig. 10, Fig. 11 and Fig. 12 show error of prediction for *LNU*, *QNU* and *CNU*. As we can see from Fig. 10 linear prediction model is relatively inaccurate because error of prediction is in a very wide range (from $-8{,}00\times10^{-3}$ to $6{,}00\times10^{-3}$ mm). This is a problem because $8{,}00\times10^{-3}$ mm of layer thickness represents 5 to 10 years of corrosion protection (although this depends on environmental influence). This is the reason why we cannot use this prediction model even to approximate calculations.

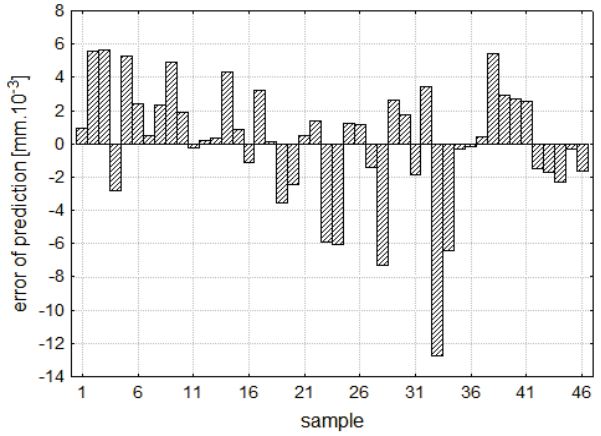

Figure 10 Validation of *LNU* for training process with 23 training data

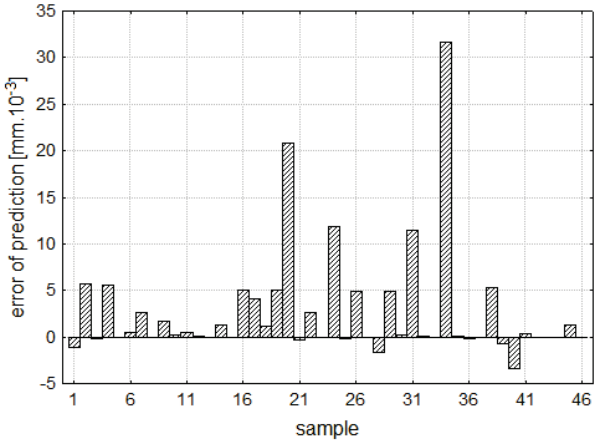

Figure 11 Validation of *QNU* for training process with 23 training data

Fig. 11 shows error of prediction of quadratic prediction model complied by *QNU*. Error of prediction for this model is mostly in toleration area 0 to $5{,}00\times10^{-3}$ mm which is a change compared to preceding situations. There are 4 big errors $21{,}00\times10^{-3}$ mm for sample 20, $12{,}30\times10^{-3}$ mm for sample 24, $12{,}20\times10^{-3}$ mm for sample 31 and $32{,}50\times10^{-3}$ mm for sample 34. These errors distort prediction too much, so quadratic prediction model is completely unusable. Cubic prediction model in Fig. 12 is useful only for approximate calculations. It is because the error of prediction has wide toleration area $\pm 4{,}00\times10^{-3}$ mm and big prediction error ($12{,}80\times10^{-3}$ mm) for sample 34.

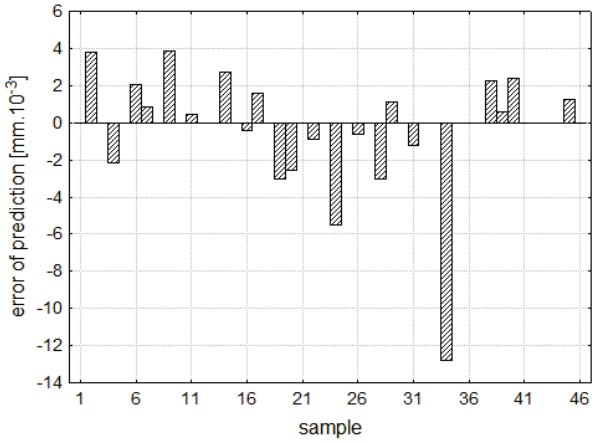

Figure 12 Validation of *CNU* for training process with 23 training data

Tab. 4 shows sum of squared errors between measured and calculated values of AAO layer thickness for each neural unit. From Tab. 4 we can conclude that examined cubic neural unit can compile very accurate prediction model if we use at least 28 training data. Cubic prediction model is considered accurate if we use at least 23 training data and prediction model can be used only for approximation if we use at least 16 training data.

Table 4 Adjustment of prediction models compiled by LNU, QNU and CNU

NoTV	Adj_{LNU} / %	Adj_{QNU} / %	Adj_{CNU} / %
46	62,74	92,77	99,93
36	61,33	57,71	99,37
28	62,50	68,05	95,97
23	54,71	69,75	79,18
16	49,68	72,67	75,76

4 Conclusion

Main objective of presented study was to create a prediction model which is able to reliably predict the resulting thickness of aluminium oxide layer, based on factors which enter the technological process of anodic aluminium oxidation. This paper shows that use of higher-order neural units has great potential for evaluation of experiments results. With properly selected range of training data, it is possible to create prediction models with reliability greater than 95 %. Such high reliability offers possibilities for off-line optimization of examined production processes. The usage of developed prediction model allows us to reduce the operating cost and simultaneously create desired value of AAO layer thickness. Finally we can state that it is possible to increase the corrosion resistance of treated components and extend their lifetime. However, use of presented algorithm also brings with it 2 significant problems:

1. It is necessary to create a preliminary computational model on which neural unit will base its learning process and subsequently control it.
2. Resulting computational model is not necessarily able to sufficiently describe controlled process and thus increases the probability for failed product.

More research should expand the prediction model by adding larger spectrum of current densities and also more precisely define influence of physical parameters on resulting AAO layer thickness.

Acknowledgement

The paper was supported by grant KEGA 026TUKE-4/2016 of Scientific Grant Agency of the Ministry of Education of Slovak Republic.

5 References

[1] Baumeister, J.; Banhart, J.; Weber, M. Aluminium foams for transport industry. // Materials &Design. 18, (1997), pp. 217-220. DOI: 10.1016/S0261-3069(97)00050-2

[2] Patermarakis, G. Development of a theory for the determination of the composition of the anodizing solution inside the pores during the growth of porous anodic Al2O3 films on aluminium by a transport phenomenon analysis. // Journal of Electroanalytical Chemistry. 447, (1998), pp. 25-41. DOI: 10.1016/S0022-0728(97)00604-9

[3] Dobrzanski, L. A.; Krupinski, M.; Sokolowski J. H. Computer aided classification of flaws occurred during casting of aluminum. // Journal of Materials Processing Technology. 167, (2005), pp. 456-462. DOI: 10.1016/j.jmatprotec.2005.05.033

[4] Kmec, J.; Fechová, E.; Hrehová, S. Diagnostics and evaluation of limit strain states from digital image. // In Latest Trends on Systems, Proceedings of the 18th International Conference on Systems, (2014), pp. 230-233

[5] Djozan, Dj.; Amir-Zehni, M. Anodizing of inner surface of long and small-bore aluminum tube // Surface & Coatings Technology. 173, (2003), pp. 185-191. DOI: 10.1016/S0257-8972(03)00510-3

[6] Aerts, T.; Dimogerontakis, T.; De Graeve, I.; Fransaer, J.; Terryn, H. Influence of the anodizing temperature on the porosity and the mechanical properties of the porous anodic oxide film. // Surface & Coatings Technology. 201, (2007), pp. 7310-7317. DOI: 10.1016/j.surfcoat.2007.01.044

[7] Evin, E.; Kmec, J.; Fechová, E. Optimizing of electric discharge texturing parameters of rolls of the rolling mill of steel sheets. // Applied Mechanics and Materials. 420, (2013), pp. 78-84. DOI: 10.4028/www.scientific.net/AMM.420.78

[8] Simunovic, G.; Svalina, I.; Simunovic, K.; Saric, T.; Havrlisan, S.; Vukelic, D. Surface roughness assessing based on digital image features. // Advances in Production Engineering & Management. 11(2016), 2, pp. 93-104. DOI: 10.14743/apem2016.2.212

[9] Park, H.S.; Nguyen, T.T.; Kim, J.C. An energy efficient turning process for hardened material with multi-criteria optimization. // Transactions of FAMENA. 40,1(2016), pp. 1-14.

[10] Michal, P.; Gombár, M.; Vagaská, A.; Piteľ J.; Kmec, J. Experimental study and modeling of the zinc coating thickness. // Advanced Materials Research. 712-715, (2013), pp. 382-386. DOI: 10.4028/www.scientific.net/amr.712-715.382

[11] Durmus, K. Prediction and control of surface roughness in CNC lathe using artificial neural network. // Journal of Materials Processing Technology. 209, (2009), pp. 3125-3137. DOI: 10.1016/j.jmatprotec.2008.07.023

[12] Hrehová, S. Informatics in quality process control. // In Automatizácia a riadenie v teórii a praxi. (2010) pp. 48-1-48-5.

[13] Simunovic G.; Simunovic K.; Saric T. Modelling and Simulation of Surface Roughness in Face Milling. // International Journal of Simulation Modelling. 12, 3(2013), pp. 141-153. DOI: 10.2507/IJSIMM12(3)1.219

[14] Banovac, E.; Kozak, D. Analysis of factors that influence micro-resistance measuring. // Strojarstvo. 52, (2010), pp. 261-270.

[15] Zárate, L. E.; Bittencout, F. R. Representation and control of the cold rolling process through artificial neural networks via sensitivity factors. // Journal of Materials Processing Technology. 197, (2008), pp. 344-362. DOI: 10.1016/j.jmatprotec.2007.06.063

[16] Gombár, M.; Vagaská, A.; Kmec, J.; Michal, P. Microhardness of the coatings created by anodic oxidation of aluminium. // Applied Mechanics and Materials. 308, (2013), pp. 95-100. DOI: 10.4028/www.scientific.net/AMM.308.95

[17] Saric T.; Simunovic G.; Simunovic K.; Svalina I. Estimation of Machining Time for CNC Manufacturing Using Neural Computing. // International Journal of Simulation Modelling. 15(2016), 4, pp. 663-675. DOI: 10.2507/IJSIMM15(4)7.359

[18] Klancnik, S.; Begic-Hajdarevic, D.; Paulic, M.; Ficko, M.; Cekic, A.; Husic, M.C. Prediction of Laser Cut Quality for Tungsten Alloy Using the Neural Network Method. // Strojniski vestnik-Journal of Mechanical Engineering. 61, 12(2015), pp. 714-720. DOI: 10.5545/sv-jme.2015.2717

[19] Chandrasekaran, M.; Devarasiddappa, D. Artificial neural network modeling for surface roughness prediction in cylindrical grinding of Al-SiCp metal matrix composites and ANOVA analysis. // Advances in Production Engineering & Management. 9, 2(2014), pp. 59-70, DOI: 10.14743/apem2014.2.176

[20] Fechová, E. The support of solving physical problem by the means of mathematical software. // Trendy ve vzdělávání 2009, 2, (2009), pp. 412-415.

[21] Fechová, E. The Use of Computer Support of Solving Problems of Probability // Trendy ve vzdělávání. 2013, 1(2013), pp. 179-182.

[22] Rodriguez, R.; Bukovsky, I.; Homma,N. Potentials of quadratic neural unit for applications. // Journal of Software Science and Computational Intelligence. 3, (2011), pp. 1-12. DOI: 10.4018/IJSSCI.2011070101

[23] Kaur, B. P.; Aggrarwal, H. An Optimization of a Planning Information System Using Fuzzy Inference System and Adaptive Neuro-Fuzzy Inference System. // WSEAS Transactions on Information Science and Applications. 10, (2013), pp. 249-260.

Authors' addresses

Alena Vagaská, PaedDr. PhD.
Faculty of Manufacturing Technologies,
Technical University of Košice,
Bayerova 1, 08001 Prešov, Slovakia
E-mail: alena.vagaska@tuke.sk

Miroslav Gombár, Ing. PhD.
Faculty of Management,
University of Prešov in Prešov,
Konštantínova 16, 08001 Prešov, Slovakia
E-mail: gombar.mirek@gmail.com